27¥
9-19-78
UC-79h

CREEP-FATIGUE LIFE PREDICTION FOR DIFFERENT HEATS OF TYPE 304 STAINLESS STEEL BY LINEAR-DAMAGE RULE, STRAIN-RANGE PARTITIONING METHOD, AND DAMAGE-RATE APPROACH

by

P. S. Maiya

BASE TECHNOLOGY

U of C-AUA-USDOE

ARGONNE NATIONAL LABORATORY, ARGONNE, ILLINOIS

The facilities of Argonne National Laboratory are owned by the United States Government. Under the terms of a contract (W-31-109-Eng-38) between the U. S. Department of Energy, Argonne Universities Association and The University of Chicago, the University employs the staff and operates the Laboratory in accordance with policies and programs formulated, approved and reviewed by the Association.

ANL-78-59

ARGONNE NATIONAL LABORATORY
9700 South Cass Avenue
Argonne, Illinois 60439

CREEP-FATIGUE LIFE PREDICTION FOR DIFFERENT HEATS OF TYPE 304 STAINLESS STEEL BY LINEAR-DAMAGE RULE, STRAIN-RANGE PARTITIONING METHOD, AND DAMAGE-RATE APPROACH

by

P. S. Maiya

Materials Science Division

July 1978

DISCLAIMER

TABLE OF CONTENTS

4

CREEP-FATIGUE LIFE PREDICTION FOR
DIFFERENT HEATS OF TYPE 304 STAINLESS STEEL BY
LINEAR-DAMAGE RULE,
STRAIN-RANGE PARTITIONING METHOD,
AND DAMAGE-RATE APPROACH

by

P. S. Maiya

ABSTRACT

The creep-fatigue life results for five different heats of Type 304 stainless steel at 593°C (1100°F), generated under push-pull conditions in the axial strain-control mode, are presented. The life predictions for the various heats based on the linear-damage rule, strain-range partitioning method, and damage-rate approach are discussed. The appropriate material properties required for computation of fatigue life are also included.

I. INTRODUCTION

For the past several years, Argonne National Laboratory has been involved in the generation of elevated-temperature, low-cycle creep-fatigue data on Type 304 stainless steel. Extensive low-cycle fatigue-test results have been generated[1] on one heat of Type 304 stainless steel (Ht 9T2796), which was produced as a reference heat for all liquid-metal fast-breeder-reactor (LMFBR) structural-component design. In contrast, the data for other heats of steel are rather limited.[2] This report summarizes the creep-fatigue data generated for five heats of Type 304 stainless steel at 593°C (1100°F) under push-pull conditions in the axial strain-control mode. Because the creep-fatigue properties of different heats can depend upon the heat treatment prior to fatigue tests, only the results obtained from heats of material with the same heat treatment are considered. Furthermore, the experimentally observed creep-fatigue life and the life predicted by the linear-damage rule, strain-range partitioning method, and damage-rate approach are compared.

II. EXPERIMENTAL MATERIAL AND PROCEDURE

The chemical compositions[3] (Table I) of the five heats of stainless steel included in the present report meet the ASTM specification. (Hereafter, only the last three digits of the heat number will be used to identify each heat.) Prior to fatigue tests, the hourglass-shape specimens were solution-annealed

in evacuated quartz tubes that were back-filled with argon for 1/2 h at 1092°C, and aged for 1000 h at 593°C. The specimens were tested in air by means of servocontrolled, hydraulically actuated fatigue machines, in the axial strain-control mode.[1,2]

TABLE I   Chemical Composition (wt %) of Various Heats
of Type 304 Stainless Steel

Elements	Heat Numbers				
	9T2796	346544	346845	X22807[a]	8043813
C	0 047	0 063	0 057	0 029	0 062
N	0 031	0 019	0 024	0 021	0 033
P	0 029	0 23	0 023	0 024	0 044
B	-	0 0002	0 0002	0 0005	0 0003
O	0 011	0 0081	0 0092	0 01	-
H	0 0006	0 0006	0 0013	0 0012	-
S	0 012	0 006	0 006	0 023	0 004
Mn	1 22	0 99	0 92	1 26	1 87
Si	0 47	0 47	0 53	0 5	0 48
Mo	0 10	0 2	0 10	0 2	0 32
Ti	0 003	0 017	0 008	0 002	0 022
Cu	0 10	0 12	0 11	0 11	-
Co	0 05	0 05	0 07	0 03	-
Pb	0 01	0 01	0 01	0 01	-
Sn	0 02	0 01	0 01	0 01	-
Ta	<0 0005	0 0006	<0 0005	<0 0005	<0 0005
Nb	0 008	0 005	0 01	0 0015	0 02
V	0 037	0 025	0 05	0 012	0 022
W	0 022	0 026	0 007	0 02	0 02
Cr	18 5	18 4	18 4	18 8	17 8
Ni	9 58	9 12	9 28	9 67	8 95
Fe	Balance	Balance	Balance	Balance	Balance

[a]Type 304L stainless steel

III. CREEP-FATIGUE LIFE RESULTS

For the reference heat of steel (Ht 796), the available data[1] include extensive continuous-cycling low-cycle fatigue data at total strain ranges from 0.35 to 2% and cyclic strain rates between 4×10^{-2} and 4×10^{-6} s^{-1}, tensile hold-time data with hold times per cycle ranging from 1 min to 10 h, and limited symmetric and compressive hold-time data for hold times varying from 1 to 10 min. Recently, new creep-fatigue data have been generated for the reference heat to establish the importance of wave-shape effects, and a detailed analysis of these data using a damage-rate approach has been presented;[4] these results are included in the present report.

For heats 544, 845, 807 and 813, the available low-cycle fatigue data are rather limited. Under continuous cycling, their fatigue lives do not differ significantly from that of the reference heat.[2] Similarly, under short symmetric and compressive hold-time conditions, all five heats have approximately the same fatigue life. However, when tensile hold times ranging from 10 to 60 min are imposed in each cycle, the creep-fatigue resistance of heats 845, 544, 807 and 813 exceeds that of the reference heat by up to a factor of three (see Fig. 1). This greater strength has been attributed to such microstructural characteristics as smaller grain size and closer spacing of grain-boundary carbides,[2] both of which result in increased resistance to grain-boundary sliding that causes initiation and growth of grain-boundary cavities during tensile hold times.
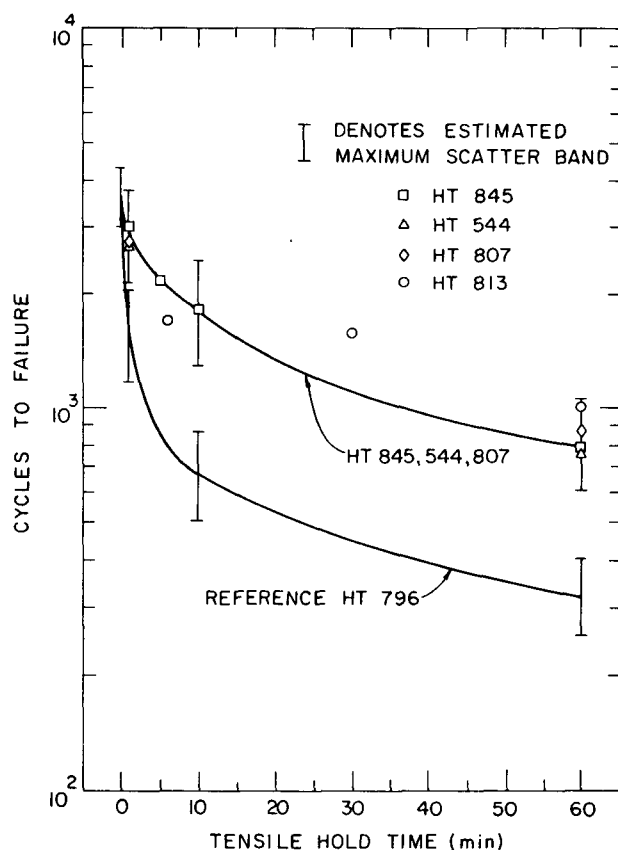
Fig. 1

Effect of Tensile Hold Time on Fatigue Life for Various Heats of Type 304 Stainless Steel at 593°C. $\Delta\varepsilon_t$ = 1%. ANL Neg. No. 306-77-278.

IV. METHODS FOR PREDICTION OF CREEP-FATIGUE LIFE

A. Linear-damage Rule

One approach to high-temperature creep-fatigue life prediction is the linear-damage rule,[5,6] based on a linear summation of cycle-dependent fatigue and time-dependent creep. For the loading cases that involve hold times at constant total strain, the linear-damage rule is

$$\frac{N_f}{N_{f0}} + N_f \int_0^{t_H} \frac{dt}{t_r} = 1,$$ (1)

where

N_f = cycles to failure,

N_{f0} = fatigue life under continuous-cycling conditions in the absence of creep,

t_H = hold time per cycle,

and

t_r = time to creep rupture in the absence of cyclic loading.

To compute creep damage by this method, monotonic creep-rupture data and stress-relaxation data are required. The time to rupture, t_r, and the stress, σ, are related by

$$t_r = M(\sigma)^{-\alpha}.$$ (2)

The parameters M and α for the reference heat and heat 845 (see Table II) were obtained from a least-squares fit of creep-rupture data to Eq. 2, with t_r in hours and σ in MPa units. The curves shown in Fig. 2 represent the regression analysis of the above data and show that heat 845 has better resistance to creep than the reference heat. The creep-rupture data for heat 845 were also used to compute life for heats 544, 807, and 813, based on the similarity in creep-fatigue behavior of these four heats.[2] The stress history during hold time for each test was obtained from the stress-relaxation behavior, which can be expressed by the equation

$$\ln(\sigma_{max}/\sigma) = \frac{B}{1+p} t^{1+p},$$ (3)

where

σ_{max} = stress at the beginning of hold time

and

B and p are parameters determined for each test (at half-life) by a least-squares fit with time, t, in min.

TABLE II. Creep-rupture Parameters for Two
Heats of Type 304 Stainless Steel

Heat No.	M	α	Remarks
796	4.535×10^{24}	9.790	$\sigma \geq 214$ MPa
	2.386×10^{20}	7.988	$\sigma \geq 214$ MPa
845	4.431×10^{30}	11.886	-
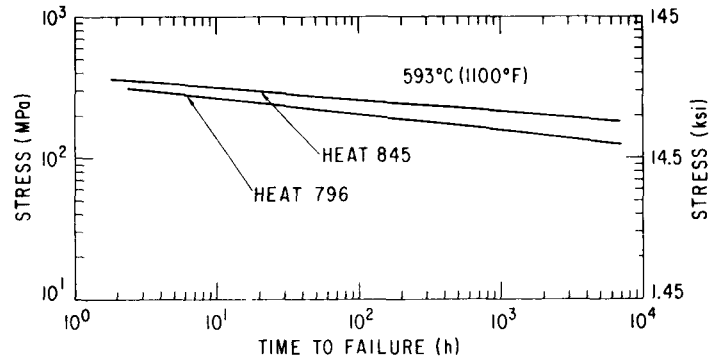
Fig. 2. Stress vs Time to Creep Rupture for Two Heats of
Type 304 Stainless Steel. ANL Neg. No. 306-77-666.

The constants B and p are listed in Tables III and IV for various heats. The continuous-cycling fatigue life required for estimation of fatigue damage is determined from the damage-rate approach.[4,7] The application of linear damage to tests involving a sawtooth waveform is not straightforward, and for the present purpose, we have assumed that only fatigue damage occurs in these loadings. Note also that the linear-damage rule as applied in Code Case 1592 assumes that the compressive hold time produces as much damage as the tensile hold time; this assumption is not realistic for austenitic stainless steels.

B. Strain-range Partitioning Method

The second approach considered in this report is the strain-range partitioning method.[8,9] In applying strain-range partitioning to several heats, only tensile hold-time data are considered because the experimental relationships for other types of loadings are not available. Also, the application of strain-range partitioning to sawtooth waveforms is not simple and hence is not considered. The interaction-damage rule for creep-fatigue loadings involving tensile hold-time periods is given by

$$\frac{1}{N_f} = \frac{F_{pp}}{N_{pp}} + \frac{F_{cp}}{N_{cp}},$$ (4)

where

$$F_{pp} = \frac{\Delta \varepsilon_{cp}}{\Delta \varepsilon_{in}},$$

$$F_{cp} = \frac{\Delta \varepsilon_{cp}}{\Delta \varepsilon_{in}},$$

$$\Delta \varepsilon_{in} = \Delta \varepsilon_{pp} + \Delta \varepsilon_{cp},$$

$\Delta \varepsilon_{pp}$ = component of inelastic strain range for which plasticity in tension is reversed by plasticity in compression,

TABLE III. Fatigue-life Prediction for Type 304 Stainless Steel--Ht 796--at 593°C

$\Delta\epsilon_t$, %	$\Delta\epsilon_p$, %	$\dot\epsilon_t$, s^{-1}	σ_t max MPa	σ_c,max, MPa	Hold Time, min	B	P	N_f Experimental	N_f Predicted by Linear-damage Rule	N_f Predicted by Strain-range Partitioning Method	N_f Predicted by Damage-rate Approach
1 0	0 714	ϵ_s 4 x 10^{-6} / ϵ_f 4 x 10^{-3}	214 1	214 1	-	-	-	261	984	-	227
1 0	0 695	ϵ_f 4 x 10^{-3} / ϵ_s 4 x 10^{-6}	228 2	228 2	-	-	-	2421	1031	-	1802
1 0	0 68	ϵ_s 1 x 10^{-4} / ϵ_f 1 x 10^{-2}	239 4	239 4	-	-	-	847	2205	-	847
1 0	0 65	ϵ_f 1 x 10^{-2} / ϵ_s 1 x 10^{-4}	261 7	261 7	-	-	-	3025	2383	-	3506
1 03	0 709	4 x 10^{-3}	242 0	246 8	2T / 2C	0 03484 / 0 04631	-0 7516 / -0 6388	2177	722	-	2574
1 0	0 706	4 x 10^{-3}	219 9	219 9	10T / 10C	0 0450 / 0 0430	-0 7250 / -0 7170	2507	766	-	924
2 048	1 638	4 x 10^{-3}	304 7	308 2	1T	0 03964	-0 8076	378	336	189	499
2 004	1 60	4 x 10^{-3}	304 1	300 6	15T	0 03139	-0 8335	237	87	149	307
1 984	1 608	4 x 10^{-3}	281 3	280 6	60T	0 02902	-0 7726	112	51	148	192
2 005	1 638	4 x 10^{-5}	269 6	279 9	60T	0 03492	-0 6809	102	65	128	103
2 024	1 672	4 x 10^{-3}	288 2	238 6	180T	0 03031	-0 7730	63	27	111	117
2 007	1 662	4 x 10^{-3}	242 0	274 4	600T	0 03159	-0 7243	87	65	97	52
0 997	0 675	4 x 10^{-3}	228 2	254 4	1T	0 0223	-0 9004	1664	2889	661	2351
1 021	0 682	4 x 10^{-3}	258 6	249 6	4C	0 01852	-0 8589	2453	718	-	3511
1 0	0 692	4 x 10^{-3}	228 2	233 0	10T	0 01938	-0 8555	706	722	743	1405
1 004	0 709	4 x 10^{-3}	218 6	222 7	15T	0 01733	-0 8812	666	758	706	1283
0 994	0 679	4 x 10^{-5}	230 3	241 3	60T	0 02765	-0 7564	305	208	501	413
1 034	0 773	4 x 10^{-3}	188 2	202 0	600T	0 0207	-0 7339	212	216	404	196
1 0	0 710	4 x 10^{-3}	214 4	219 4	600T	0 2111	-0 7889	242	72	425	194
0 595	0 365	4 x 10^{-3}	167 6	177 2	15T	0 01429	-0 9011	2765	4759	2116	3553
0 598	0 346	4 x 10^{-5}	182 2	194 2	60T	0 02468	-0 7924	1031	1098	1465	1118
0 594	0 38	4 x 10^{-3}	152 4	168 9	180T	0 01336	-0 9161	1284	1782	1759	1417
0 55	0 331	4 x 10^{-3}	154 3	173 5	60T	0 009487	-0 8972	1253	2219	3332	2869
0 503	0 272	4 x 10^{-3}	162 7	182 0	10T	0 01249	-0 6754	3803	3574	6567	4705
0 356	0 13	4 x 10^{-5}	164 8	173 7	10T	0 01243	-0 5113	11412	4235	16240	8629
1 0	0 707	4 x 10^{-3}	228 2	210 3	15T / 5C	0 05496 / 0 08408	-0 8265 / -0 6772	1788	1633	-	1300
2 0	1 618	4 x 10^{-3}	298 5	273 0	15T / 5C	0 04038 / 0 05211	-0 8541 / -0 7863	642	172	-	390

Heat No	$\Delta\varepsilon_t$ %	$\Delta\varepsilon_p$, %	$\dot{\varepsilon}_t$ s^{-1}	σ_t, max MPa	σ_c max MPa	Hold Time, min	B	P	N_f Experimental	N_f Predicted by Linear-damage Rule	N_f Predicted by Strain-range Partitioning Method	N_f Predicted by Damage-rate Approach[a]	N_f Predicted by Damage-rate Approach[b]
845	1 003	0 666	4×10^{-3}	253 4	245 9	1T	0 02342	-0 791	3034	3267	1072	2931	3117
845	1 027	0 702	4×10^{-3}	240 0	246 3	5T	0 02162	-0 8221	2222	2793	784	2054	2307
845	0 99	0 683	4×10^{-3}	226 8	232 5	10T	0 01667	-0 8458	1826	2864	886	2027	2315
845	1 0	0 743	4×10^{-5}	195 8	195 0	60T	0 02902	-0 6465	767	946	476	516	597
845	1 03	0 70	4×10^{-3}	253 9	241 2	1C	0 02887	-0 7789	2747	3284	-	3452	3452
845	0 987	0 659	4×10^{-3}	244 8	243 9	2C	0 01658	-0 8703	2659	3384	-	3777	3777
845	1 0	0 677	4×10^{-3}	247 6	236 6	4C	0 03150	-0 7206	2997	3095	-	3494	3494
845	1 0	0 699	4×10^{-3}	230 6	224 2	10C	0 02083	-0 7851	2624	2828	-	3275	3275
845	0 994	0 666	4×10^{-3}	240 5	249 5	1T	0 06048	-0 5885	2880	3015	-	2652	2807
						1S	0 008191	-0 8985					
845	0 99	0 674	4×10^{-3}	238 6	235 0	2T	0 04228	-0 7940	2348	3402	-	2735	2735
						2C	0 04247	-0 7698					
544	1 0	0 672	4×10^{-3}	248 5	247 5	1T	0 01324	-0 9160	2712	3533	820	3035	3198
544	1 02	0 675	4×10^{-5}	236 5	272 8	60T	0 02647	-0 7273	751	860	507	550	648
544	1 02	0 697	4×10^{-3}	241 9	234 7	4C	0 02074	-0 7938	2366	2922	-	3383	3383
807	0 99	0 698	4×10^{-3}	223 3	213 3	1T	0 03728	-0 7369	2755	3461	934	2621	2801
807	1 01	0 745	4×10^{-5}	213 0	183 9	60T	0 02538	-0 6905	874	884	507	571	647
807	1 019	0 730	4×10^{-3}	216 8	215 9	4C	0 01983	-0 8202	2603	3088	-	3127	3127
813	1 02	0 674	4×10^{-3}	254 0	264 1	1T	0 01715	-0 8629	2529	3293	967	2864	3049
813	0 993	0 651	4×10^{-5}	243 4	268 2	60T	0 02955	-0 7061	1034	872	464	559	663

[a] k_c = 0 55
[b] k_c = 0 60

$\Delta \varepsilon_{cp}$ = component of inelastic strain range for which creep in tension is reversed by plasticity in compression,

$\Delta \varepsilon_{in}$ = total inelastic strain range,

N_{pp} = cyclic life associated with a given $\Delta \varepsilon_{pp}$ strain range,

and

N_{cp} = cyclic life associated with a given $\Delta \varepsilon_{cp}$ strain range.

The strain-range partitioning relationships for N_{pp} and N_{cp} for the reference heat are expressed by[10]

$$\ell n \; N_{pp} = 16.044 - (219.2958 + 32.7858 \; \ell n \; \Delta \varepsilon_{pp})^{1/2} \tag{5}$$

$$N_{cp} = 1.0322 \times 10^{-3}(\Delta \varepsilon_{in})^{-2.0903}. \tag{6}$$

Similar relationships for other heats are not available; therefore the relationships established for the reference heat are used for all the other heats of material. The stress-relaxation parameters listed in Tables III and IV are used for computing "cp" strains.

C. Damage-rate Approach

The third approach used for the analysis of creep-fatigue data from all five heats of Type 304 stainless steel is the damage-rate approach. As.this method has been discussed in detail in Ref. 4, only its essential ingredients are outlined below.

The damage-rate approach addresses two major types of damage in materials subjected to creep, fatigue, and creep-fatigue loadings: namely, crack damage and cavity damage. Crack damage contributes to failure through crack initiation at the surface and its subsequent propagation. Cavity damage contributes to failure through grain-boundary cavity initiation and growth. Thus, creep-fatigue failure depends on the relative amounts of these two types of damage and their interaction, and is significantly influenced by the type of creep-fatigue loadings and the microstructural characteristics of the material. The basic damage equations[4] are

$$\frac{1}{a}\frac{da}{dt} = \begin{cases} T\,|\varepsilon_p|^m\,|\dot{\varepsilon}_p|^k & \text{for tension} \\[2mm] C\,|\varepsilon_p|^m\,|\dot{\varepsilon}_p|^k & \text{for compression} \end{cases} \tag{7}$$

and

$$\frac{1}{c}\frac{dc}{dt} = \begin{cases} G|\epsilon_p|^m|\dot{\epsilon}_p|^{k_c} & \text{for tension} \\ \\ -G|\epsilon_p|^m|\dot{\epsilon}_p|^{k_c} & \text{for compression,} \end{cases} \qquad (8)$$

where

a = current crack size,

c = current cavity size,

$|\epsilon_p|, |\dot{\epsilon}_p|$ = absolute values of current plastic strain and strain rate, respectively,

and

T, C, G, m, k, and k_c are material parameters that are functions of temperature, environment, and microstructure.

The interaction between crack and cavity damage is assumed[4] to be of the form

$$\frac{\ln(a/a_0)}{\ln(a_f/a_0)} + \frac{\ln(c/c_0)}{\ln(c_f/c_0)} = 1 \qquad (9)$$

where

a_0, c_0 = initial crack size and cavity size, respectively,

a_f = final crack size in a specimen free of cavities,

and

c_f = final cavity size in a specimen free of cracks (related to spacing of cavities).

Whenever $c \leq c_0$, it is assumed that the cavities anneal out, so that $c > c_0$. Thus, negative net cavity damage is not allowed, although the incremental cavity damage can be negative. The damage-rate equations can be integrated[4] to compute life for various loading paths such as continuous cycling, monotonic creep rupture, and loadings that involve sawtooth waveforms and hold times; the results are given in the appendix. The damage-rate parameters, $A \left[A = \dfrac{T + C}{2} \Big/ \ln\left(\dfrac{a_f}{a_0}\right) \right]$, k, m, $C_g \left(C_g = \dfrac{G}{\ln c_f/c_0} \right)$, k_c, and T/C (see Eqs. 7-9) are established without the use of any hold-time data and are shown in Table V.[2,4]

14

TABLE V. Material Parameters of the Damage-rate Approach

Heat No.	A	m	k	C_g	k_c	T/C
796	2.52	1	0.74	0.73	0.55	4
544, 807, 845, 813	2.52	1	0.74	0.73	0.60	4

Unlike the strain-range partitioning method, the damage-rate approach incorporates the rate effect in the damage-accumulation process; it does so without separating the total inelastic strain into different components, and it does not resort to back-fitting of hold-time fatigue data. The relationship between the damage-rate approach and other methods, such as Coffin's frequency-modified approach[11,12] and the strain-range partitioning method, is shown by the fact that both the frequency-modified life and strain-range partitioning relationships can be derived from the damage-rate approach.[7] Also, the damage-rate approach can take into account the loading-sequence effects where the cavity damage incurred during the part of the fatigue life with tensile hold times can anneal out during subsequent loadings involving compressive hold times.[13] Some of the fundamental differences among the various approaches to creep-fatigue life prediction have important practical implications, especially in the extrapolation of the existing data base to regions where experimental data do not exist.[14]

V. COMPARISON OF EXPERIMENTAL AND PREDICTED RESULTS

The fatigue-life prediction results for various heats of Type 304 stainless steel at 593°C (1100°F) obtained by the linear-damage rule, strain-range partitioning method, and damage-rate approach are shown in Tables III and IV and Figs. 3-5. The dashed lines in Figs. 3-5 indicate deviation of the predicted life from the experimental life by a factor of two. Ignoring the accuracy of fitting, most of the available experimental data are predicted reasonably well, from a design viewpoint, by all three methods. The linear-damage rule (see Fig. 3) yields nonconservative results for loading cases that involve a sawtooth waveform. Also, in Fig. 4, where only the tensile hold-time fatigue data are considered and the microstructural effects of different heats are ignored, the calculated life for heats 845, 544, 807, and 813 (based on material-property data for the reference heat) underpredicts the experimentally observed life. This is also true if the damage-rate approach is used.[2]

The differences in creep-fatigue behavior between the reference heat 796 and the other heats (845, 544, 807, and 813) cannot be explained on the basis of stress-relaxation behavior, as all the heats are characterized by the same plastic-strain history during hold times. Figure 6 is based on the strain-range partitioning method and shows the importance of strain-rate effects. If

Fig. 3

Fatigue–life Prediction for Various Heats of Type 304 Stainless Steel by the Linear–damage Rule. T = tension, S = symmetric, C = compression. ANL Neg. No. 306–77–662.

Fig. 4

Fatigue–life Prediction for Various Heats of Type 304 Stainless Steel by the Strain–range Partitioning Method. T = tension. ANL Neg. No. 306–77–663.
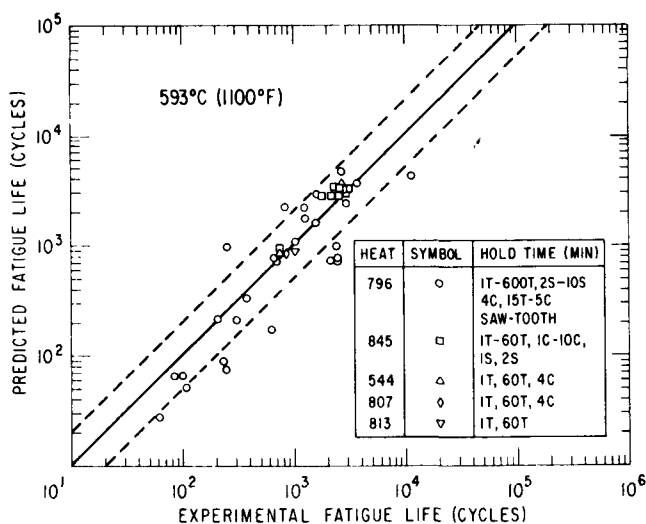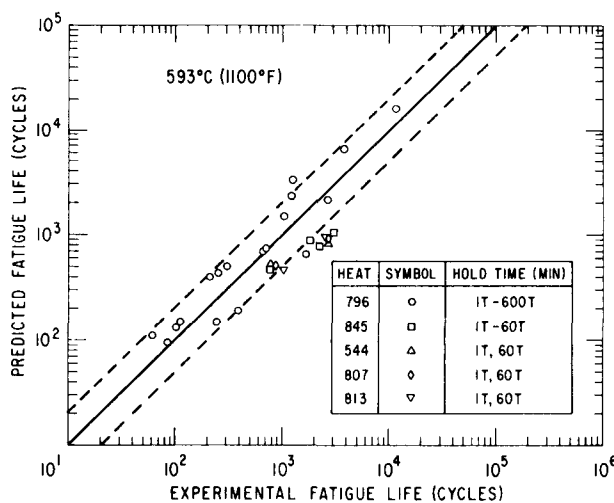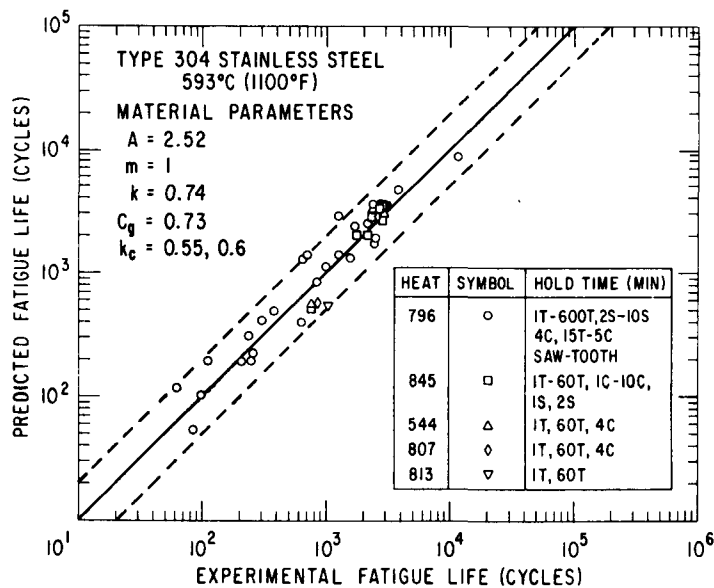

Fig. 5

Fatigue–life Prediction for Various Heats of Type 304 Stainless Steel by the Damage–rate Approach. T = tension, S = symmetric, C = compression; k_c = 0.55 for the reference heat and 0.6 for the other heats of steel. ANL Neg. No. 306–77–659.
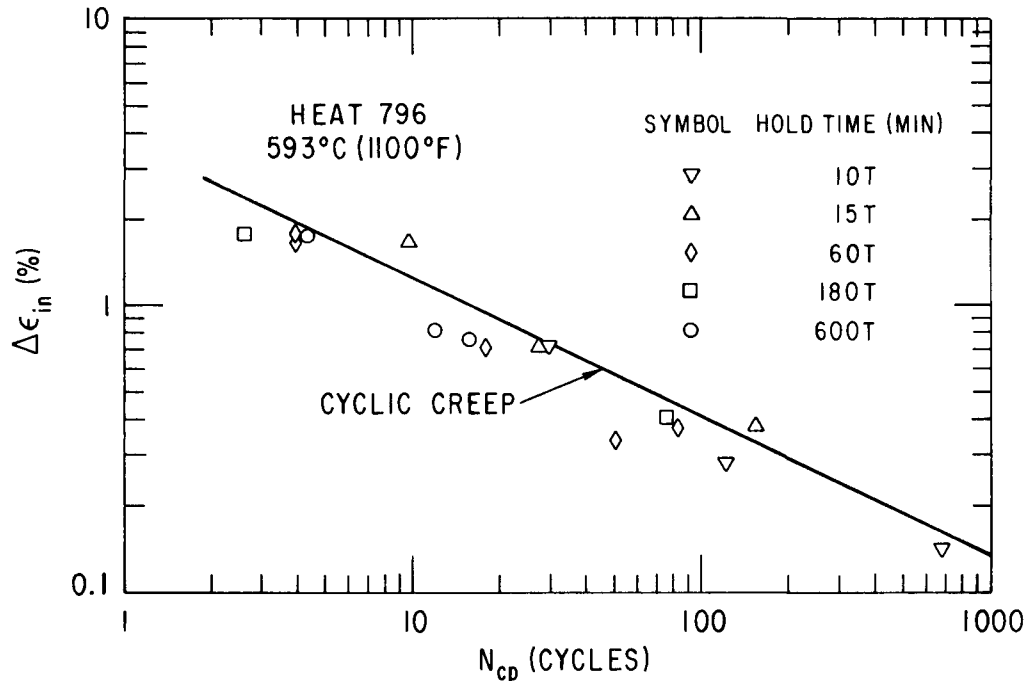
Fig. 6. Plot of $\Delta\varepsilon_{in}$ vs N_{cp} for Reference Heat of Type 304 Stainless Steel. The solid line is generated from cyclic–creep data; the symbols represent cyclic–relaxation data. ANL Neg. No. 306–77–664.

strain-range partitioning relationships based on cyclic-creep data are used to predict cyclic-relaxation fatigue lives, the results tend to be nonconservative. Similar conclusions have been reached using the damage-rate approach.[7] The prediction of fatigue life for different heats by the damage-rate approach partially takes into account the microstructural effects, which result in different values of k_c for the reference heat and the other heats.

More accurate life predictions can be achieved by establishing the value of the "cavity-damage parameter" C_g for the heats that exhibit superior creep-fatigue strength. Since heats 845, 544, 807, and 813 are more resistant to intergranular fracture than the reference heat, the value of C_g for these heats is expected to be smaller than that of the reference heat. The present report uses the value of C_g established for the reference heat for the other heats. Finally, the interaction between crack and cavity damage is described[4] in a simple form (Eq. 9) and requires further investigation.

VI. CONCLUSIONS

A study of three methods for creep-fatigue life prediction, using the available data for five different heats of Type 304 stainless steel, shows that

the greatest divergence between the experimental and calculated life results when the linear-damage rule is used. The available short tensile hold-time data for different heats can be predicted reasonably well by the strain-range partitioning method and the damage-rate approach. However, strain-range partitioning, unlike the damage-rate approach, depends heavily on the hold-time data for life prediction. Furthermore, the application of the linear-damage rule and strain-range partitioning to sawtooth waveforms is not straightforward. The damage-rate approach treats tensile, creep, and creep-fatigue deformation in a unified manner.

The creep-fatigue and material-property data included in the present report should serve as a guide for the critical examination of existing and new creep-fatigue interaction models as they develop with further understanding of creep-fatigue damage. Also, the long-term cyclic-relaxation tests (especially those at low strain ranges) initiated at Argonne National Laboratory should facilitate evaluation of the existing models for use in the design of structural components.

APPENDIX[4]

Equations for Computing Life for Various Loading Paths
Using Damage-rate Approach

1. Continuous-cycling Case

$$N_f = \frac{m+1}{4A}\left(\frac{\Delta\epsilon_p}{2}\right)^{-(m+1)}\dot{\epsilon}_p^{1-k}, \qquad (A.1)$$

where the parameters A, m, and k can be determined from a least-squares fit of continuous-cycling data to Eq. A.1.

2. Monotonic Creep Rupture

$$t_r = \left(\frac{m+1}{f_1+f_2}\right)^{1/(m+1)}\dot{\epsilon}_p^{-(k_c+m)/(1+m)}, \qquad (A.2)$$

where

$$t_r = \text{time to rupture,}$$

$$f_1 = \left(T'\Big/\ln\frac{a_f}{a_0}\right)\dot{\epsilon}_p^{k-k_c},$$

$$f_2 = \frac{G'}{\ln(C_f/C_0)},$$

and

T' and G' = the parameters in the damage-rate equations. (The prime is used to distinguish from the cyclic case.)

For creep tests at low stress or strain rate, $f_2 \gg f_1$, so that

$$t_r \propto \dot{\epsilon}_p^{-(k_c+m)/(1+m)}.$$

Therefore, on a log-log plot, the slope of time-to-rupture versus plastic strain rate is $-(k_c + m)/(1 + m)$; thus k_c can be determined from the creep-rupture data.

3. Sawtooth Waveform: Fast-Slow

$$N_f = \frac{m+1}{4A}\left(\frac{\Delta\epsilon_p}{2}\right)^{-(m+1)}\left(\frac{\dot{\epsilon}_f^{k-1}}{1+C/T}+\frac{\dot{\epsilon}_s^{k-1}}{1+T/C}\right)^{-1}, \qquad (A.3)$$

where

$$\dot{\epsilon}_f = \text{fast tensile plastic strain rate}$$

and

$$\dot{\epsilon}_s = \text{slow compressive plastic strain rate.}$$

The T/C ratio can be determined from the above equation by correlation with the results of fast-slow fatigue tests. The cavity damage for this case is zero.

4. Sawtooth Waveform: Slow-Fast

$$N_f = \left\{ \frac{4A}{m+1} \left(\frac{\Delta\epsilon_p}{2}\right)^{m+1} \left(\frac{\dot{\epsilon}_s^{k-1}}{1+C/T} + \frac{\dot{\epsilon}_f^{k-1}}{1+T/C}\right) \right.$$

$$\left. + \frac{2C_g}{m+1} \left(\frac{\Delta\epsilon_p}{2}\right)^{m+1} \left(\dot{\epsilon}_s^{k_c-1} - \dot{\epsilon}_f^{k_c-1}\right) \right\}^{-1}, \qquad (A.4)$$

where

$$\dot{\epsilon}_s = \text{slow tensile plastic strain rate,}$$

$$\dot{\epsilon}_f = \text{fast compressive plastic strain rate,}$$

and

$$C_g = \frac{G}{\ln(C_f/C_o)}.$$

5. Hold-time Fatigue

$$N_f = \frac{1}{d_T + d_C}, \qquad (A.5)$$

where

$$d_T = \frac{4A}{m+1} \left(\frac{\Delta\epsilon_p}{2}\right)^{m+1} \dot{\epsilon}_p^{k-1} + \frac{2A}{1+C/T} \int_0^{t_t} |\epsilon_p|^m |\dot{\epsilon}_p|^k \, dt$$

$$+ \frac{2A}{1+T/C} \int_0^{t_c} |\epsilon_p|^m |\dot{\epsilon}_p|^k \, dt, \qquad (A.6)$$

$$d_C = C_g \int_0^{t_t} |\epsilon_p|^m |\dot{\epsilon}_p|^{k_c} \, dt - C_g \int_0^{t_c} |\epsilon_p|^m |\dot{\epsilon}_p|^{k_c} \, dt, \qquad (A.7)$$

$$t_t = \text{tensile hold time,}$$

and

$$t_c = \text{compressive hold time.}$$

ACKNOWLEDGMENT

I would like to thank S. Majumdar for helpful discussions.

REFERENCES

1. D. R. Diercks and D. T. Raske, *Elevated-temperature, Strain-controlled Fatigue Data on Type 304 Stainless Steel: A Compilation, Multiple Linear Regression Model, and Statistical Analysis*, ANL-76-95 (Dec 1976).

2. P. S. Maiya and S. Majumdar, *Elevated-temperature Low-cycle Fatigue Behavior of Different Heats of Type 304 Stainless Steel*, Metall. Trans. A *8A*, 1651-60 (1977).

3. V. K. Sikka, H. E. McCoy, Jr., M. K. Booker, and C. R. Brinkman, *Heat-to-Heat Variation in Creep Properties of Types 304 and 316 Stainless Steels*, J. Pressure Vessel Technol. *96*, 243-51 (1975).

4. S. Majumdar and P. S. Maiya, "Wave-shape Effects in Elevated-temperature Low-cycle Fatigue of Type 304 Stainless Steel," in *Inelastic Behavior of Pressure Vessel and Piping Components*, eds. T. Y. Chang and E. Krempl, PVP-PB-028, American Society of Mechanical Engineers, pp. 43-54 (1978).

5. E. L. Robinson, *Effect of Temperature Variation on the Long-time Rupture Strength of Steels*, Trans. ASME *74*(5), 777-781 (1952).

6. D. A. Spera, *Calculation of Thermal-fatigue Life Based on Accumulated Creep Damage*, NASA Technical Note, NASA-TN-D-5489 (1969).

7. S. Majumdar and P. S. Maiya, "A Unified and Mechanistic Approach to Creep-Fatigue Damage," pp. 924-28 in *Proc. 2nd Int. Conf. Mechanical Behavior of Materials*, ICM-II, American Society for Metals, Metals Park, Ohio (1976). See also ANL-76-58 (Jan 1976).

8. S. S. Manson, G. R. Halford, and M. H. Hirschberg, "Creep-fatigue Analysis by Strain-range Partitioning," pp. 12-28 in *Design for Elevated Temperature Environment*, American Society of Mechanical Engineers, New York (1971).

9. S. S. Manson, "The Challenge to Unify Treatment of High Temperature Fatigue--A Partisan Proposal Based on Strain-range Partitioning," pp. 744-82 in *Fatigue at Elevated Temperatures*, ASTM STP 520, American Society for Testing and Materials, Philadelphia (1973).

10. D. R. Diercks, "The Application of Strain Range Partitioning to the Prediction of Elevated-temperature, Low-cycle Fatigue Life for Type 304 Stainless Steel," pp. 29-38 in *Advances in Design for Elevated Temperature Environment*, American Society of Mechanical Engineers, New York (1975).

11. L. F. Coffin, "Predictive Parameters and Their Application to High Temperature, Low-cycle Fatigue," pp. 643-54 in *Fracture 1969: Proc. 2nd Int. Conf. on Fracture*, Chapman and Hall, London (1969).

12. L. F. Coffin, *The Effect of Frequency on the Cyclic Strain and Low Cycle Fatigue Behavior of Cast Udimet 500 at Elevated Temperature*, Met. Trans. *2*, 3105-13 (1971).

13. S. Majumdar and P. S. Maiya, "Hold-time-sequence Effects on Elevated-temperature Low-cycle Fatigue of Type 304 Stainless Steel," to be presented at *Winter Annual Meeting of the ASME*, San Francisco (Dec 1978).

14. S. Majumdar, *Importance of Strain Rate in Elevated-temperature Low-cycle Fatigue of Austenitic Stainless Steels*, Nuclear Engineering and Design (to be published).

Distribution of ANL-78-59

Internal:

J. A. Kyger	H. O. Monson	S. Majumdar
R. Avery	R. Sevy	K. L. Merkle
L. Burris	R. W. Weeks	M. H. Mueller
D. W. Cissel	L. T. Lloyd	R. B. Poeppel
S. A. Davis	J. F. Schumar	D. T. Raske
B. R. T. Frost	E. Stefanski (2)	K. J. Reimann
D. C. Rardin	T. H. Blewitt	R. W. Siegel
R. J. Teunis	M. B. Brodsky	D. Stahl
C. E. Till	W. J. Shack	H. R. Thresh
R. S. Zeno	F. Y. Fradin	H. Wiedersich
C. E. Dickerman	A. G. Hins	D. R. Diercks
H. K. Fauske	T. F. Kassner	A. B. Krisciunas
S. Fistedis	U. F. Kocks	ANL Contract File
B. D. LaMar	P. S. Maiya (10)	ANL Libraries (5)
J. F. Marchaterre		TIS Files (6)

External:

DOE-TIC, for distribution per UC-79h (274)
Manager, Chicago Operations Office
Chief, Office of Patent Counsel, CH
Director, Reactor Programs Div., CH
Director, CH-INEL
Director, DOE-RRT (2)
President, Argonne Universities Association
Materials Science Division Review Committee:

    E. A. Aitken, General Electric Co., Sunnyvale
    G. S. Ansell, Rensselaer Polytechnic Inst.
    R. W. Balluffi, Massachusetts Inst. Technology
    R. J. Birgeneau, Massachusetts Inst. Technology
    S. L. Cooper, U. Wisconsin
    C. Laird, U. Pennsylvania
    M. T. Simnad, General Atomic
    C. T. Tomizuka, U. Arizona
    A. R. C. Westwood, Martin Marietta Labs.